

RF performance projections for 2D Graphene Transistors: Role of Parasitics at the Ballistic transport limit

Pei Zhao^{1*}, Debdeep Jena¹, and, Siyuranga O. Koswatta²

¹ Department of Electrical Engineering, University of Notre Dame, Notre Dame, IN 46556, USA

² IBM Research Division, T. J. Watson Research Center, Yorktown Heights, NY 10598, USA

Phone: (574)631-1290 Email: *pzhao@nd.edu

Background: Graphene is a two-dimensional zero bandgap material with carbon atoms arranged in a honeycomb lattice [1, 2]. Although 2D monolayer graphene lacks a bandgap, it still shows promising potential for applications in high frequency analog devices that do not require a high on/off ratio as demanded by digital logic [3-5]. A cutoff frequency, f_T , as high as 170GHz is achieved in a 90 nm channel length Graphene Field-Effect-Transistor (GFET) with back-gated structure [4]. Projected $f_T = 300$ GHz is reported for channel length $L_{ch} = 140$ nm top-gated structure [5]. The motivation of this work is to explore the potential of high frequency performance of GFETs, and to elucidate the major factors that limit their performance. Our model captures the degradation of intrinsic performance due to parasitics, and the effect of metal-graphene (M-G) contacts as: (1) contact doping effect due to M-G work function difference [6], and (2) DOS broadening by M-G coupling and metal-induced states in the channel [7, 8].

Model: The simulations in this work utilize a mode-space based non-equilibrium Green's function formalism for ballistic transport with self-consistent electrostatics. The 2D electrostatics is solved by a finite-difference method. A channel width of 150nm is assumed, and the 2D graphene Hamiltonian matrix is decoupled into 1D modes. The q th mode retarded Green's function is $G_q(E) = [(E+i0^+)I - H_q - \Sigma_{Sq} - \Sigma_{Dq}J^{-1}]^{-1}$, and $\Sigma_{Sq}^{l,l} = (t_0)^2 g_{Sq}$, $t_0 = 3$ eV. The surface Green's function is $g_{Sq}(E) = [(E+i\Delta)I - H_{contact}J^{-1}]^{-1}$, where Δ is the M-G coupling strength [7,8]. Inside the M-G contact, the Fermi level of the graphene layer under the metal electrode shifts by $\Delta E_{contact} = E_F - E_{Dirac}$ [6] which is captured in the electrostatic solution.

Results and discussions: The modeled device structures are shown in Figure 1, (a) top-gated structure $\epsilon_{ox} = 20$ and $t_{ox} = 1.5$ nm, and (b) back-gated structure with 90nm thick SiO₂. The contact resistance and parasitic capacitance have also been taken into consideration in the simulations. Figure 2 shows the effect of M-G contacts on the transfer characteristics and transconductance, g_m for the top-gated structure. The on-current, I_{on} , can be increased with strong M-G coupling strength Δ or heavy contact induced doping (i.e. larger $\Delta E_{contact}$). The off-current, I_{off} , does not increase. Large $\Delta E_{contact}$ increases g_m , but the maximum g_m does not show a strong dependence on Δ . We use $\Delta = 50$ meV and $\Delta E_{contact} = -0.4$ eV for rest of the simulations. Figure 3 shows the I_{DS} vs. V_{GS} and g_m vs. V_{GS} at different V_{DS} for the top-gated structure. Large V_{DS} yields a higher maximum g_m , but low V_{DS} shows better linearity with a broader f_T peak. Transfer characteristics with different channel lengths are shown in Figure 4. For the top-gated structure excellent gate electrostatics helps avoid short channel effects (SCE). I_{on} remains the same for all channel lengths. I_{off} increases about 1.5 times when L_{ch} decreases from 100nm to 15nm due to direct source to drain tunneling. The rise in I_{off} leads to g_m degradation at $L_{ch} = 15$ nm. In the back-gated structure, the on/off ratio is degraded at shorter channel lengths, and the minimum conduction point shifts. Figure 5 shows the effect of contact resistance on $I_D - V_{GS}$ characteristics at $L_{ch} = 100$ nm. At $V_{DS} = 0.3$ V, compared with the intrinsic case, when $R_{SD} = 0.5$ Ω mm, on/off ratio decreases 3x for the top-gated structure and 1.2x for the back-gated structure. I_{on} reduces 22x for the top-gated structure and 6x for the back-gated structure. Figure 6 shows the comparison of $f_T - V_{GS}$ with different channel lengths at $V_{DS} = 0.3$ V. The cutoff frequency is calculated as $f_T = 1/2\pi\tau_{tot}$, where $\tau_{tot} = L_{ch}C_{gs}/g_m + C_{gd}/g_m + C_{gd}(R_S + R_D)$, $C_{gs} = \partial Q_{ch}/\partial V_{GS}$, $R_{SD} = 0.5$ Ω mm, and $C_{gd} = 2$ pF/cm and 0.5pF/cm for the top-gated and the back-gated structures, respectively. Charging/discharging process is faster at shorter channel lengths, thus the peak f_T increases. In the back-gated structure, SCE is strong, thus the on/off ratio decreases and g_m drops dramatically at short L_{ch} . When L_{ch} is shorter than 30nm, even the peak f_T drops. Figure 7 summarizes the f_T vs. L_{ch} at $V_{DS} = 0.3$ V. The intrinsic $f_T = \langle v \rangle / 2\pi L_{ch}$ is added as a reference with the average ballistic velocity $\langle v \rangle = 2v_F/\pi$ in 2D graphene. With $R_{SD} = 0.5$ Ω mm and $C_{gd} = 2$ pF/cm, f_T drops 2x at $L_{ch} = 100$ nm and 8x and $L_{ch} = 15$ nm for the top-gated structure. For the back-gated structure, with $R_{SD} = 0.5$ Ω mm and $C_{gd} = 0.5$ pF/cm, when L_{ch} is below 70nm, f_T does not increase, and it even decreases when the channel length is below 30nm. Thus, parasitics currently dominate the performance, and major gains are expected with their reduction. This work is supported by the Semiconductor Research Corporation Nanoelectronics Research Initiative and the National Institute of Standards and Technology through the Midwest Institute for Nanoelectronics Discovery (MIND).

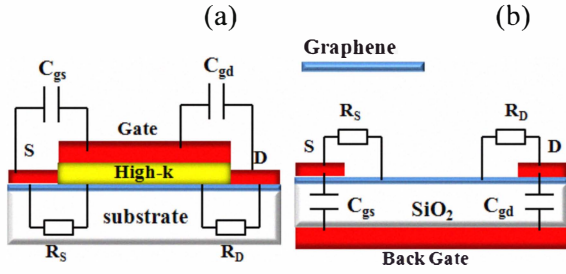


Figure 1. Modeled device structure with contact resistances and parasitic capacitances. (a) top-gated structure, $\epsilon_{ox} = 20$ and $t_{ox} = 1.5\text{nm}$ and (b) back-gated structure with 90nm thick SiO_2 .

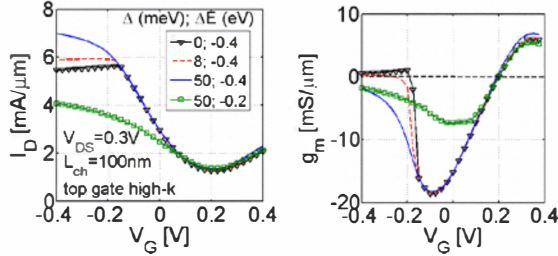


Figure 2. Effect of contact induced doping and metal/graphene coupling Δ . I_{on} can be increased with strong coupling Δ and high contact doping $\Delta E_{contact}$. I_{off} will keep the same with different Δ . Maximum g_m shows strong dependence on $\Delta E_{contact}$.

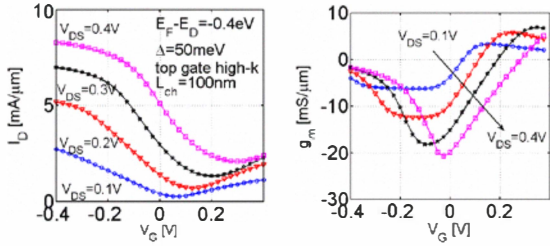


Figure 3. I_{DS} vs. V_G and g_m vs. V_G for the top-gated structure. Large V_{DS} gives higher maximum g_m , but low V_{DS} shows better linearity with broader f_T peak.

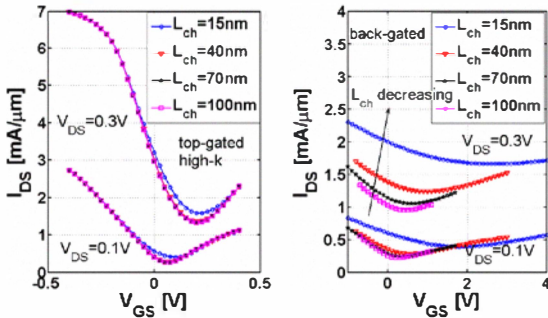


Figure 4. Transfer characteristics at different channel length for both device structures. For the top-gated structure with excellent gate electrostatics, I_{on} remains the same, and I_{off} increases about 1.5 times. For the back-gated structure, short channel effect is strong and the minimum conduction point shifts with different channel lengths.

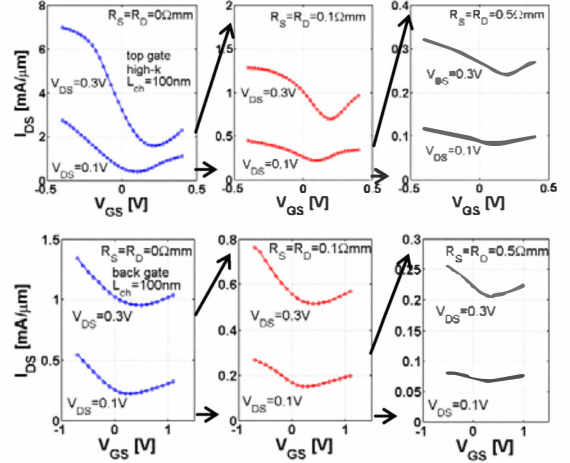


Figure 5. Effect of contact resistances on the transfer characteristics. The increase of contact resistance, dramatically reduces the on/off ratio and I_{on} .

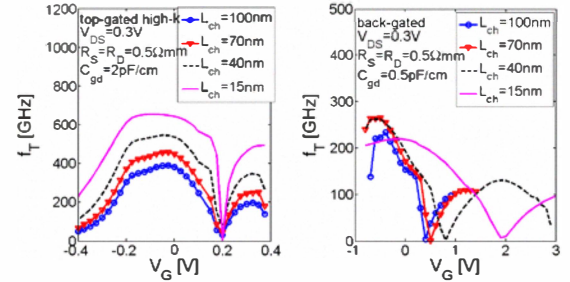


Figure 6. Effect of R_{SD} and C_{gd} on cut-off frequency f_T vs. V_G with different channel lengths. For the top-gated structure, peak f_T increases while channel lengths is shrinking, but for the back-gated structure, peak f_T drops when $L_{ch} < 30\text{nm}$.

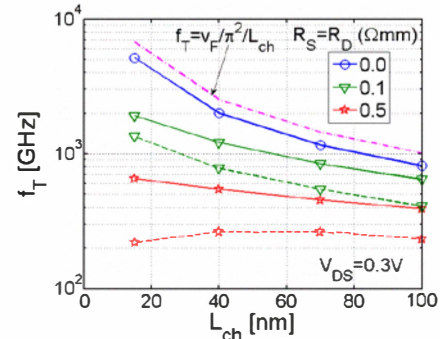


Figure 7. Prediction of peak f_T with the impact of contact resistances and parasitic capacitances (solid lines for the top-gated structure, $C_{gd} = 2\text{pF/cm}$ and dashed lines for the back-gated structure, $C_{gd} = 0.5\text{pF/cm}$). With $R_{SD} = 0.5\Omega\text{mm}$ and $C_{gd} = 2\text{pF/cm}$, f_T drops 2x at $L_{ch} = 100\text{nm}$ and 8x and at $L_{ch} = 15\text{nm}$ for the top-gated structure. For the back-gated structure, with $R_{SD} = 0.5\Omega\text{mm}$ and $C_{gd} = 0.5\text{pF/cm}$, when $L_{ch} < 70\text{nm}$, f_T does not increase, in addition, f_T even drops for L_{ch} below 30nm.